The pAblo·pCasso self-curing vector toolset for unconstrained cytidine and adenine base-editing in *Pseudomonas* species

by

Ekaterina Kozaeva[1], Zacharias S. Nielsen[1], and Pablo I. Nikel[1]*

[1] The Novo Nordisk Foundation Center for Biosustainability, Technical University of Denmark, 2800 Kgs. Lyngby, Denmark

Keywords: Base-editing; CRISPR; PAM-less; Cas9; Metabolic engineering; Synthetic biology; *Pseudomonas*

Running title: Unconstrained base-editing in *Pseudomonas*

* Correspondence to: Pablo I. Nikel (pabnik@biosustain.dtu.dk)
The Novo Nordisk Foundation Center for Biosustainability,
Technical University of Denmark
Kgs. Lyngby 2800, Denmark
Tel: (+45) 93 51 19 18

ABSTRACT

Pseudomonas species are platforms for chemical production. To unleash their potential as cell factories, we designed synthetic biology tools based on clustered regularly interspaced short palindromic repeats (CRISPR) and CRISPR-associated protein 9 (Cas9) base-editors. A cytidine base-editor (CBE) and an adenine base-editor (ABE) were tailored for high-resolution genome engineering. CBE involves a cytidine deaminase fused to a nickase Cas9 from *Streptococcus pyogenes* (^{Sp}nCas9) variant that converts cytidine to uracil, resulting in a C→T (or G→A) substitution. ABE relies on an adenine deaminase fused to a nickase ^{Sp}nCas9 variant to enable A→G (or T→C) editing. We established plasmid-borne, base-editing systems for efficient nucleotide substitution using a novel protospacer adjacent motif (PAM)-relaxed ^{Sp}nCas9 (SpRY) variant. Base-editing was demonstrated by introducing premature *STOP* codons in target genes (encoding both fluorescent proteins and metabolic functions), resulting in functional knockouts (using CBE). The wild-type genotype was recovered by eliminating the engineered *STOP* codons (using ABE). *P. putida* could be base-edited at ca. 75-95% efficiency for both types of editors. Furthermore, a set of induction-dependent vectors enabled efficient curing of the plasmid-based editing platform in a single, 8-h cultivation step. This strategy eases complex strain construction programs independently of homologous recombination and yields plasmid-free engineered cells.

GRAPHICAL ABSTRACT

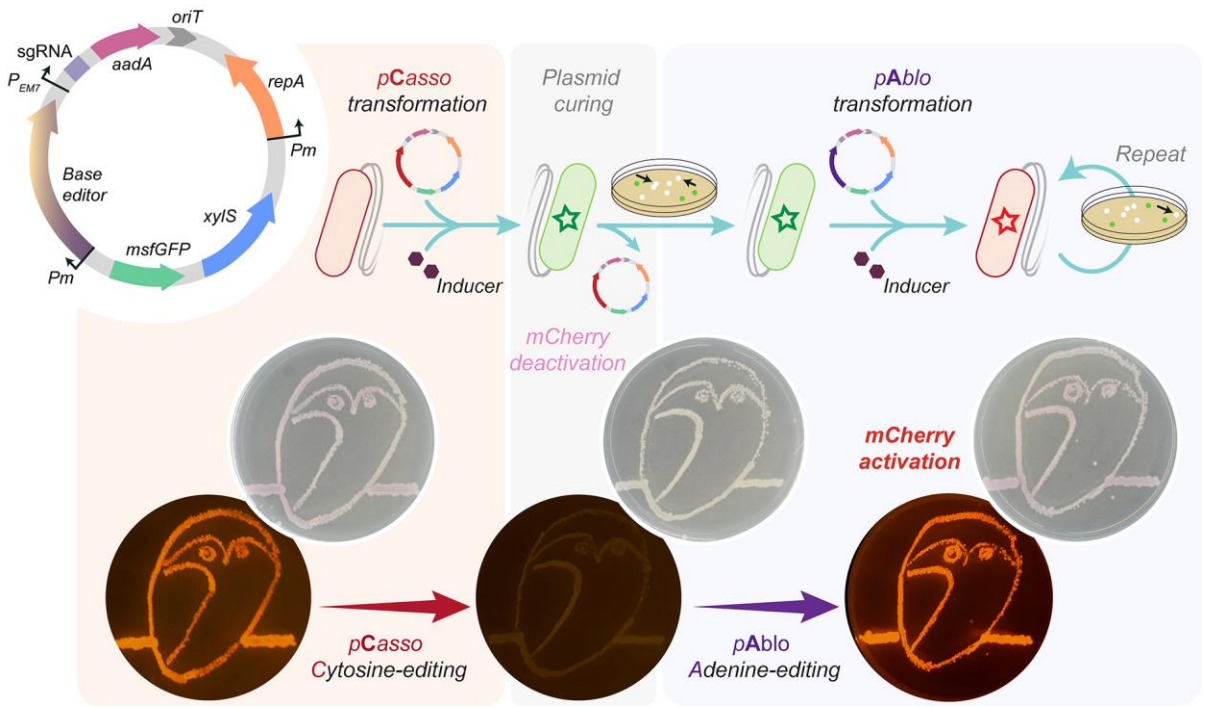

INTRODUCTION

Genome editing continues to revolutionize life sciences, with a direct impact in multiple fields of application [1,2]—including both fundamental studies and metabolic engineering [3,4]. Among these emerging approaches, base-editing of bacterial genomes, assisted by modified Cas proteins associated with clustered regularly interspaced short palindromic repeats (CRISPR), allows for the single-nucleotide-resolution modification of genomic sites in a homologous recombination-independent fashion [5-8]. Such DNA engineering techniques rely on synthetic editing modules—most commonly, cytidine base-editors (CBE) that result in a cytidine (C)→thymidine (T) [or guanine (G)→adenine (A)] substitution, and adenine base-editors (ABE) that enable A→G (or T→C) modifications [9]. A CBE typically carries a cytidine deaminase fused to a Cas9 nickase (nCas9) and uracil glycosylase inhibitors [10], and an ABE consists of an nCas9 and an evolved adenine deaminase, capable of recognizing single-stranded DNA (ssDNA) [11]. In the type-II CRISPR-Cas system, the naturally-occurring CRISPR-associated enzyme 9 from *Streptococcus pyogenes* (^{Sp}Cas9) recognizes its targets with the help of the cognate guide, formed as a complex of a transactivating crRNA (tracrRNA) and a small RNA molecule (crRNA), transcribed from the CRISPR array [12]. Serving as a defense system from invading nucleic acid fragments, a CRISPR array functions as a library containing spacers, adapted from sequences located next to specific short sequences called protospacer-adjacent motifs (PAMs). PAM is required for binding of the Cas9 domain to the target sequence [13]. In the system engineered for base-editing, after binding to a compatible PAM, nCas9 catalyzes a single strand break (owing to the presence of the D10A mutation in the RuvC cleavage domain of ^{Sp}Cas9, which blocks double-stranded DNA breaks). The cleavage is introduced in a sequence matching a spacer borne by a synthetic single-guide RNA (sgRNA), and this target recognition process is constrained by the identity of the PAM sequence [14]. ^{Sp}Cas9 recognizes the 5'-*N*GG-3' motif, where *N* can be any nucleotide. From a practical point of view, the PAM recognition profile constrains CRISPR targeting efforts, leaving numerous genome loci inaccessible to editing—e.g. regions with low G+C content. To tackle this issue, DNA-binding CRISPR proteins were optimized for flexible PAM recognition [8]. These engineered variants hold great potential for improved genome editing as they render more DNA sites accessible to several types of modifications. Hence, fusing such proteins with nucleotide deaminase domains provides a unique opportunity for modification of almost any DNA base of choice without strict PAM recognition. Developing this type of base-editing methodology is especially relevant for microbial strain engineering, as it allows for fast genome modifications along the bacterial

chromosome. PAM-independent base-editing by CBEs enables the integration of premature *STOP* codons into an open reading frame (ORF), such that 5'-CAG-3', 5'-CAA-3' or 5'-CGA-3' codons can be converted into 5'-TAG-3' (amber), 5'-TAA-3' (ochre) or 5'-TGA-3' (opal) triplets, respectively—thereby inactivating the target protein function (i.e. functional knockout). Likewise, these modifications could be reverted to restore the original (coding) sequence of the target ORFs using ABEs, providing for a functional switch in genome modifications. Partial attempts to develop these technologies have been made in model bacterial organisms, e.g. *Escherichia coli* [15,16], the availability of base-editing tools for alternative microbial hosts (e.g. *Pseudomonas* species) is restricted to a few exploratory examples.

Pseudomonas species are essential microbial models for both fundamental and applied research. Several *Pseudomonas* isolates are known to tolerate high levels of abiotic stress, e.g. oxidative damage and solvents, underscoring their potential as biotechnological hosts. *Pseudomonas putida*, for instance, displays a rich and versatile metabolism that renders this species an ideal platform for metabolic engineering [17,18]. While some clinically-relevant species, e.g. *Pseudomonas aeruginosa*, are a frequent cause of nosocomial complications in immunosuppressed patients, other *Pseudomonas* are plant pathogens that can infect a variety of commercially-relevant crops [19]. Genome engineering tools have advanced *Pseudomonas* research, linking phenotypes to genotypes and unraveling the metabolic impact brought about by genome alterations [20,21]. Tools for gene deletion, insertion and genome modification are well established for *P. putida*—but these techniques are tedious, time-consuming and difficult-to-automate [22]. Non-homologous end joining (NHEJ) mechanisms are virtually absent in prokaryotes, preventing the introduction of frameshifts in target ORFs—and functional knock-outs thereof. Proof-of-principle studies on CRISPR/Cas-assisted editing in *Pseudomonas* species revealed promising results on the use of this approach for genome engineering [23-25].

On this background, in this work we demonstrated a novel application of the engineered nearly-PAM-less ^{Sp}Cas9 variant (SpRY) for nucleotide substitution in Gram-negative bacterial systems and developed a plasmid toolset (termed pAblo·pCasso) for efficient base-editing. Different types of editor modules (i.e. CBE and ABE) were characterized using both canonical ^{Sp}nCas9 and nearly PAM-less SpRY. SpRY can target almost all PAMs in the genome (5'-*NRN*-3' being preferable to 5'-*NYN*-3', where R is A or G and Y is C or T). A set of induction-dependent, self-curing and standardized vectors, displaying conditional replication for easy plasmid curing, was created to complement the set of tools for metabolic engineering

applications. A detailed, step-by-step protocol for base-editing and plasmid curing is presented to this end. The genome editing methods developed here, combined with efficient vector curing, simplifies genetic manipulations in *Pseudomonas* species and has the potential to accelerate the pace of a wide variety of studies involving these non-model organisms.

MATERIALS AND METHODS

Bacterial strains, plasmids and culture conditions

Bacterial strains and plasmids used in this study are listed in **Table 1**. *E. coli* and *P. putida* cultures were grown in lysogeny broth (LB) medium (10 g L^{-1} tryptone, 5 g L^{-1} yeast extract and 10 g L^{-1} NaCl; solid culture media additionally contained 15 g L^{-1} agar) at 37ºC and 30ºC, respectively. Streptomycin (Str) was added whenever needed at 100 μg mL^{-1} (for *E. coli* cultures) or 200 μg mL^{-1} (for *P. putida* cultures). Nicotinic acid was added to culture media at 5 mM for experiments involving base-editing of the *nicX* gene. Liquid cultures were agitated at 200 rpm (MaxQ™ 8000 incubator; ThermoFisher Scientific, Waltham, MA, USA). The optical density measured at 600 nm (OD_{600}) was recorded in a Genesys 20 spectrophotometer (ThermoFisher Scientific) to estimate bacterial growth. For preculture preparation, four colonies were picked from an LB plate and used to inoculate wells of a 96-deep well plate filled with 1 mL of LB supplemented with the appropriate antibiotic(s). Bacterial growth, mCherry fluorescence ($\lambda_{excitation}/\lambda_{emission}$ = 567 nm/610 nm) and msfGFP fluorescence ($\lambda_{excitation}/\lambda_{emission}$ = 475 nm/510 nm) were measured along the experiment in a Synergy HI plate reader (BioTek Instruments, Inc., Winooski, VT, USA). Unless stated otherwise, cultivations were performed in 96-well microtiter plates with a flat bottom and a lid; basal fluorescence levels of *P. putida* KT2440 were subtracted from the individual readings. For physiological characterization of engineered strains, growth kinetics were derived from OD_{600} readings with the light path correction in an ELx808 plate reader (Buch and Holm A/S, Herlev, Denmark) under constant shaking.

General cloning procedures and construction of plasmids

Oligonucleotides used in this work are listed in **Table S1** in the Supplementary Information. Unless stated otherwise, uracil-excision (*USER*) cloning [26] was used for the construction of all recombinant plasmids;

the *AMUSER* tool was employed for designing oligonucleotides [27]. Phusion™ *U* high-fidelity DNA polymerase (ThermoFisher Scientific) was used according to the manufacturer's specifications in PCR amplifications intended for *USER* cloning. For colony PCR, the commercial *OneTaq*™ master mix (New England BioLabs, Ipswich, MA, USA) was used according to the supplier's instructions. *E. coli* DH5α λ*pir* (**Table 1**) was employed as a host for general cloning purposes. Chemically-competent *E. coli* cells were prepared and transformed with plasmids using the *Mix and Go*™ commercial kit (Zymo Research, Irvin, CA, USA) according to the manufacturer's indications. Electrocompetent *P. putida* cells were prepared by washing the biomass from LB medium cultures with 300 mM sucrose, followed by transformation with plasmids by electroporation [28]. The sequence of all used plasmids was verified by Mix2Seq sequencing (Eurofins Genomics, Ebersberg, Germany).

Editing events confirmation by Sanger sequencing

Eight to 24 identified positive clones of each strain were picked, and inoculated into 5 mL of LB medium added with the proper antibiotic(s). After overnight (~16 h) cultivation, cultures were subjected to plasmid isolation using the NucleoSpin™ Plasmid EasyPure kit (Macherey-Nagel, Dueren, Germany) or colony PCR using Q5™ High-Fidelity 2× Master Mix (New England Biolabs) if a chromosomal region was targeted. Either the isolated plasmids or the purified PCR products were Sanger-sequenced using the Mix2Seq kit (Eurofins Scientific, Luxembourg) with a respective set of primers (**Table S1**); the obtained sequences were analyzed and visualized using Benchling (Biology software 2021).

Plasmid copy number analysis by quantitative PCR (qPCR) and fluorescence-based counting assays

Plasmid copy number analysis was performed essentially according to the protocol of Fernández-Cabezón et al. [29]. To this end, a qPCR approach was set in a QuantStudio™ 5 Real-Time PCR system (ThermoFisher Scientific). Expression levels of the *aadA* gene, encoding an aminoglycoside adenylyltransferase that mediates Str resistance, were calculated and converted to the copy number of plasmids carrying the gene. The empty pSEVA448 vector (**Table 1**), was used as a reference for these experiments. Plasmid DNA was purified using NucleoSpin™ Plasmid EasyPure kit (Macherey-Nagel) according to manufacturer's instructions, and the plasmid suspensions were diluted to 1-10 ng μL^{-1} to

build calibration curves. *P. putida* cells containing different plasmids as indicated in the text were grown for 10 h in 96-well plates until the cultures reached mid-exponential phase (OD_{600} ~ 0.5). Samples were collected from each well, diluted with phosphate buffered saline (PBS) to contain 1×10^3 cells per sample and stored at –20°C until the analysis was carried out. All qPCR amplifications were performed under the following conditions: 50°C for 2 min, 95°C for 10 min, followed by 40 cycles consisting of 95°C for 15 s, 60°C for 1 min and 72°C for 30 s. Each experiment included a non-template control (i.e. a mixture of primers with water, and a mixture of primers with the reaction mix but without any plasmid). Three technical replicates were run for each biological sample; results were analyzed in QuantStudio™ design and analysis software (ThermoFischer Scientific). A comparative $2^{-\Delta\Delta Ct}$ method [30] was applied to calculate gene copy number by comparing ΔΔCt values of the analyzed *P. putida* clones to the ΔΔCt values of calibration curves.

Fluorescence-based assessment of plasmid loss was done with a 50-μL aliquot of each bacterial culture recovered after the base-editing procedure. The OD_{600} of these samples was normalized to 0.5 for each strain and the suspension was plated onto LB medium agar plates supplemented with 100 μg mL^{-1} Str and 1 mM of 3-methylbenzoate (3-*mBz*) as an inducer of the XylS/*Pm* system. All plates were covered by aluminum foil and incubated at 30°C for 24 h to allow for sufficient bacterial growth; after cultivation, total colonies in each plate were counted in an automated UVP ColonyDoc-It imaging station (Analytik Jena US LLC, Upland, CA, USA) with a trisection protocol. Non-fluorescent *P. putida* colonies in each of all three zones were further counted with and without blue light in a transilluminator (ThermoFisher Scientific). The efficiency of plasmid curing (ρ) was calculated as the number of non-fluorescent colonies in each zone divided for the total number of visible colonies in the same zone.

Flow cytometry analysis of bacterial cells

Flow cytometry analysis was performed in a Miltenyi MACSQuant™ VYB flow cytometer (Miltenyi Biotec Norden AB, Lund, Sweden), using medium-mixing and fast running mode. In these experiments, 1,000–10,000 events were recorded for each sample. Bacterial cells were gated for singlets in exponential phase, and events within the singlet gate were recorded for each well and each condition analyzed. Median fluorescence values of each triplicate (consisting of a minimum of 5,000 events) were calculated as indicated previously [31]. The FlowLogic™ software (Inivai Technologies, Victoria, Australia) was used

for analysis and data interpretation. Base-editing efficiency was additionally confirmed by sequencing of 10-30 individual colonies isolated as indicated in each experimental setup.

Data and statistical analysis

All figures were created using Adobe Illustrator (Adobe Inc., San Jose, CA, USA); graphics and plots were generated using the Prism 9 GraphPad software (Boston, MA, USA). All the experiments reported in this study were independently repeated at least three times with individual biological replicates (as indicated in the corresponding figure or table legend), and the mean value of the corresponding parameter ± standard deviation is presented. Data analysis of qPCR and flow cytometry results was assisted by R programming using RStudio and customized flowCore R scripts [32]; mean values ± standard deviations were exported to Prism 9 GraphPad for visualization. When relevant, the level of significance of differences when comparing results across experiments was evaluated by ANOVA (Bartlett's test) with a P value < 0.01.

RESULTS AND DISCUSSION

Tailoring cytidine and adenine base-editors for precision nucleotide substitution in *P. putida*

The use of ^{Sp}Cas9 variants free of PAM restrictions has emerged as a powerful option for DNA base-editing in both fundamental and applied research due to significantly improved target accessibility. Among the nucleases described thus far, an evolved ^{Sp}Cas9 nickase variant (termed SpRY) enabled nearly PAM-less genome engineering in human cells [8], zebrafish [33], plants [34] and yeast [35]. In this work, SpRY was adopted as the basis to tailor a set of base-editors towards pushing the PAM-restriction boundaries in bacterial base-editing engineering. SpRY contains 11 specific amino acid changes as compared to the wild-type ^{Sp}Cas9 nuclease (**Table S2**, Supplementary Information). As indicated above, SpRY allows for the recognition of alternative PAMs, with a preference towards 5'-*N*R*N*-3' (R = A or G) sites over 5'-*N*Y*N*-3' motifs (Y = C or T) [8], while remaining similarly efficient towards the canonical 5'-*N*GG-3' PAM.

A CBE, which allows cytidine (C•G) to thymine (T•A) substitutions (**Fig. 1A**), and an ABE, which converts adenine (A•T) to guanine (G•C) (**Fig. 1B**), were adopted in this study. A CBE typically encompasses three functional components [9], i.e. a cytidine deaminase (APOBEC1), fused to a catalytically-impaired ^{Sp}Cas nickase and two copies of the gene encoding an uracil glycosylase inhibitor (UGI) from *Bacillus subtilis* bacteriophage PBS1, which efficiently inhibits counterproductive DNA repair processes [10,24]. The ABE, on the other hand, contains two components, i.e. an evolved adenine deaminase, TadA, an *E. coli* tRNA^{ARG}-modifying enzyme, capable of recognizing ssDNA, and a ^{Sp}Cas nickase [11]. In order to avoid the limitations traditionally associated with the narrow base-editing window of ABEs and their generally low editing efficiencies, we chose the ABE8.20-m module, encoding an evolved ABE of the ABEmax8 generation (ABEmax, **Fig. 1B**). This synthetic ABE displays increased activity, improved Cas compatibility, broadened base-editing window and, owing to these properties, this base-editor has been deemed suitable even for therapeutic applications [36].

With these functional parts at hand, we proceeded to build a plasmid-borne set of base-editors as follows. Firstly, all of the genetic elements of the base-editors previously applied in mammalian cell engineering were repurposed for their use in bacterial systems. In this case, DNA fragments were synthesized *de novo* to encode SpRY (nicking variant, carrying an additional D10A mutation), APOBEC1, 2UGI and ABEmax. Each of these DNA segments was codon-optimized to facilitate expression in Gram-negative bacteria and cured from restriction sites as outlined in the Standard European Vector Architecture (SEVA) framework [37,38]. The SEVA platform is a user-friendly plasmid system that facilitates standardization in synthetic biology, based on swapping and combining individual genetic modules (e.g. promoters, origins of replication and antibiotic selection markers), to expand the options for genome engineering in Gram-negative bacteria (including *P. putida*). We used the pMCRi vector series, previously developed in our team for CRISPR interference in *P. putida* [28], as the physical template of the base-editing toolbox, and we exchanged the gene encoding ^{Sp}dCas9 (a catalytically inactive Cas9 protein) with the respective base-editor module. All oligonucleotide and gene sequences used for these constructs are presented in **Tables S1** and **S2** in the Supplementary Information, respectively. These modifications gave rise to a subset of base-editing, SEVA-compatible vectors (**Table 1**): pEditC (carrying a CBE, based on the canonical nicking ^{Sp}nCas9), pEditA (bearing an ABE, based on the canonical nicking ^{Sp}nCas9), pEditC-RY (with a CBE and the evolved nicking SpRY) and pEditA-RY (with an ABE and the evolved nicking

SpRY). The next step was to test the functionality of these base-editing plasmids in *P. putida*, as disclosed in the next section.

Cytidine and adenine base-editors enable gene modifications at single-nucleotide resolution in *P. putida* when using a canonical PAM motif

The Cas9-based editing system requires a specific 20 nucleotide spacer sequence in the sgRNA, which determines the navigation of the ^{Sp}nCas9 protein and DNA nicking (ssDNA break) in the genomic target to be modified. **Fig. 2A** shows an example of a sgRNA sequence binding to the non-coding strand of the gene, encoding the mCherry fluorescent protein. This spacer for gRNA must be selected specifically for each DNA target as a 20 nucleotide sequence followed by a PAM motif. The canonical PAM sequence for ^{Sp}Cas9 is 5'-*N*GG-3', whereas for an engineered SpRY variant, the GG duplet can be preferably replaced with any combination of GA, AG or AA—or even other nucleotides, if an alternative design is not possible. An important aspect of the spacer design is to choose unique sequences in the bacterial genome to be edited to avoid off-target effects (**Fig. 2B**). To ensure that this is the case, a BLAST analysis [39] against the complete genomic DNA sequence of the target strain should reveal no obvious sequence similarities: the lack of homology in the seed sequence of the sgRNA, comprising 8-10 bases at the 3'-end of the sgRNA targeting sequence, usually suffices to avoid unintended ^{Sp}nCas9 binding [40,41]. The efficiency of base-editing also depends on the identity of the nucleotides adjacent to the target residue. For instance, the optimal sequence preferred for CBE activity is 5'-[**T**C ≥ **C**C ≥ **A**C > **G**C]-3' with the target C nucleotide in the second position, whereas for ABE activity the preference is 5'-[**T**A ≥ **G**A ≥ **A**A > **C**A]-3' with the target A nucleotide in the second position [9,42].

The vectors described in this study (i.e. plasmids pEditA, pEditC, pEditA-SpRY and pEditC-SpRY; **Table 1**) contain two *Bsa*I (*Eco*31I) recognition sites that are placed upstream of the sgRNA construct. Further linearization of the selected plasmid with *Bsa*I allows for the integration of the unique target-specific spacer, which can be assembled as a duplex of two oligonucleotides that are complementary to each other. This duplex displays *Bsa*I-compatible overhangs for easy ligation into the vector. In particular, one oligonucleotide should contain the 20-nt spacer sequence from the target ORF, flanked at the 5'-end with a 5'-GCGCG-3' motif; another oligonucleotide should be its reverse complement with the addition of a 5'-AAAC-3' sequence to the 5'-end and a 'C' nucleotide at the 3'-end. For example, to edit the Q47 codon

of the *mCherry* gene by means of the synthetic CBE (**Fig. 2A**), we used the following oligonucleotides to create a duplex *via* direct annealing: CBE_F_*mCherry*^{Q47} (5'-GCG CG**C ACC CAG ACC GCC AAG CTG A**-3') and CBE_R_*mCherry*^{Q47} (5'-AAAC **TCA GCT TGG CGG TCT GGG TG**C-3') (**Table S1**, Supplementary Information). The unique spacer sequence is shown in bold in these oligonucleotides, where the reverse sequence is complementary to the target DNA. After verifying the plasmid identity and correctness by DNA sequencing, we transformed these vectors into bacteria containing the *mCherry* gene in different configurations to test the base-editors functionality.

To compare the editing performance of the nCas9 or SpRY-based cytidine editors in *P. putida,* we first used spacers with canonical PAM sequences targeting the *mCherry* gene. In particular, we targeted the cytidine residues of codons Q47 and W64 towards creating premature *STOP* codons and thus block gene translation (**Fig. 2A**). We tested the editing efficiency for both types of editors in *P. putida* strain KT·YFP·mCherry (**Table 1**), carrying an *mCherry* gene integrated in the chromosome. This engineered *P. putida* strain, previously constructed in our lab [28], expresses the *YFP* and *mCherry* genes under control of the synthetic P_{EM7} promoter—conferring constitutive red fluorescence to be used for proof-of-concept manipulations. This reporter system enables simple screening of base-editing efficiency, as the inactivation of the *mCherry* gene through the introduction of a premature *STOP* codon in the fluorescence marker ORF would lead to non-fluorescent bacterial cells.

P. putida KT·YFP·mCherry (mCherry^{+}) was transformed with derivatives of vectors pEditC (i.e. nCas9-based editor) or pEditC-RY (i.e. SpRY-based editor), both endowed with constitutively expressed gRNAs carrying target-specific Q47 or W64 spacers, adjacent to 5'-*N*GG-3' canonical PAMs. Specifically, plasmids pEditC·*mCherry*^{Q47}, pEditC·*mCherry*^{W64}, pEditC-RY·*mCherry*^{Q47} and pEditC-RY·*mCherry*^{W64} (**Table 1**) were individually delivered into *P. putida* KT·YFP·mCherry to generate edited strains. After incubating the cells for 1 h, a 1-μL aliquot of the transformation culture was inoculated in 10 mL of LB medium and further incubated at 30°C for 24 h. The bacterial culture was then diluted with PBS buffer (to reach a density of 1×10^3 cells per sample) and analyzed by flow cytometry based on mCherry fluorescence; the base-editing efficiency was estimated based on the population-wide shift of red fluorescence values between control experiments and cells transformed with the editing plasmids indicated above (**Fig. S1A**, Supplementary Information). In these experiments, comparing native and engineered nucleases, SpRY and ^{Sp}nCas9 showed a similar editing performance for canonical PAMs

(**Fig. 2C**). The observed spacer-dependent variation in editing efficiency (i.e. Q47 was edited to a *STOP* codon in 85-95% of the cells and W64 was edited in 75-85% of the bacterial population), is determined by the spacer thereof, but not the Cas9 variant nature.

While the chromosome-encoded *mCherry* gene could be efficiently silenced by using the base-editors engineered herein, we were also interested in testing base-editing in a multicopy target format. To this end, we tested the editing performance of the target gene, located on the multicopy plasmid for both types of editors in *P. putida* KT2440 (wild-type strain) carrying plasmid pS2313·*mCherry* (**Table 1**). This plasmid encodes the same reporter construct previously used for chromosome-based expression (i.e. P_{EM7}→*mCherry*) in a vector backbone carrying the low-copy-number *oriV*(RK2) replicon [29,43]. When strain KT2440/pS2313·*mCherry* was transformed with the base-editor plasmids (**Table 1**) and subjected to the same flow cytometry analysis explained above, we observed a clear shift in the red fluorescence levels for all the resulting strains. A small fraction of mCherry-free *P. putida* cells could be observed in these cultures (ca. 8-10%), together with an additional sub-population displaying a low mCherry signal (**Fig. S1B**, Supplementary Information). Taken together, these results indicate that the *in situ* plasmid editing occurred with 40-60% efficiency for both ^{Sp}nCas9 and SpRY—yielding bacterial populations with heterogeneous levels of mCherry fluorescence. Even though the overall base-editing capacity for multiple gene copies dropped by ca. 20% (as compared to single-copy gene modifications), the activity of the ^{Sp}nCas9 and SpRY remained comparable—with a sufficiently high efficiency for further applications. Thus, we concluded that both proteins have similar efficacy in nucleotide substitution while targeting the classical (5'-*N*GG-3') PAM motif.

Cytidine and adenine base-editing with non-canonical PAM sequences in *P. putida*

The next step was to test SpRY activity in *P. putida* using spacers with non-canonical PAMs, which would result in an expanded preference to 5'-*N*RR-3' motifs (where *N* is any nucleotide and R is either adenine or guanine). Based on the results described in the previous section, we compared both types of base-editors in strain KT·YFP·mCherry, carrying an integrated *mCherry* gene in the *att*Tn7 site in the chromosome [28]. We targeted the *START* codon of *mCherry* using 3 different spacers with varying PAM motifs: M1-1 (5'-AGG-3', which corresponds to the canonical PAM sequence), M1-2 (5'-GAG-3') and M1-3 (5'-CGA-3') (**Fig. 2D**). If successful, the resulting base substitution would result in an alternative *START*

codon [5'-GTG-3' [44]] for *mCherry*. Alternative *START* codons are known to affect the levels of protein formation and transcription strength of the ORF [45], and they have been implemented to study the dependence of transcription activity on the Shine-Dalgarno sequence [46].

We tested base-editing profiles for both types of editors in *P. putida* KT·YFP·mCherry, transformed with plasmids pEditA and pEditA-RY, carrying the adenine base-editors, and 3 different spacers (i.e. M1-1, M1-2 and M1-3; i.e. pEditA·*mCherry*^{M1}-1-3 and pEditA-RY·*mCherry*^{M1}-1-3, **Table 1**). Similarly to the previous experiments, 1 μL of the bacterial transformation mixture was inoculated in 10 mL of LB medium, and the cells were grown at 30°C for 24 h. Upon plating the bacterial suspension on LB agar plates, single colonies were isolated, picked and used for PCR analysis followed by DNA sequencing. Visual inspection of the plates indicated that most of the colonies retained the red fluorescence phenotype at different levels, while some colonies were non-fluorescent (data not shown). The base-editing efficiency with the M1-1 spacer, encompassing the canonical 5'-NGG-3' PAM, was very high for both ^{Sp}nCas9 and SpRY (>95% in both cases). As expected, only the evolved SpRY protein showed activity when using the M1-2 and M1-3 spacers (i.e. carrying the 5'-NRR-3' PAM). The base-editing efficiency observed in these cases (~92-95%) was comparable to that observed for the M1-1 spacer (**Fig. 2D**). When the bacterial population was analyzed by flow cytometry based on mCherry fluorescence, we could further confirm the absence of any ^{Sp}nCas9 activity against the M1-2 and M1-3 spacers—while *P. putida* cells edited with the SpRY variant showed a clear phenotype with all spacers tested (**Fig. S2A-C**, Supplementary Information). Interestingly, replacing the *ATG* codon by the (in principle, weaker) *GTG START* codon resulted in a rather heterogeneous population in all the edited strains, characterized by a fraction of bacteria devoid of mCherry and sub-populations that accumulated different amounts of the fluorescent marker—in some cases, even higher than those observed in the positive, non-edited control strain. This observation can be accounted by the Shine-Dalgarno dynamics in relation to translation-initiation, which may improve protein expression and counteract mRNA secondary structures [45].

One way or the other, the results so far show that SpRY can access new non-canonical PAM sequences (i.e. M1-2 and M1-3) in Gram-negative bacteria, whereas the ^{Sp}nCas9 protein is not able to recognize these motifs. These observations indicate that SpRY is a promising addition to the synthetic biology toolbox for base-editing and other CRISPR-Cas9 related applications. It can expand the spectrum of genome-editing possibilities in bacterial systems by making more targets in the genome accessible. To

provide a more robust vector for editing manipulations, we further decided to improve the plasmid toolkit in *P. putida* by engineering inducer-dependent plasmid curing as explained below.

Medium- and high-copy-number vectors with conditional replication allow for efficient, one-step curing of plasmids

Plasmid-borne genome editing has a bottleneck that has been rarely addressed thus far in the literature: upon obtaining the desired genotype, the plasmid needs to be quickly cured from the modified strain towards downstream applications or to allow for further editing events using different spacers or types of editors. Hence, we addressed vector 'curability' after the DNA editing process based on the plasmid-borne ABE and CBE toolbox. Generally, plasmid-curing is accomplished by repetitive dilution and passaging of the cells in a culture media with no selection pressure (i.e. antibiotic), and screening of single colonies isolated from non-selective solid media to select for antibiotic sensitivity [47]. An efficient vector-curing approach was recently developed for *Pseudomonas* species [48]. Based on the conditional control of *trfA* expression, this system facilitates inducer-dependent replication of vectors based on the low-copy-number *oriV*(RK2) origin of replication. While this approach has been successfully implemented for metabolic engineering, low-copy-number vectors are not ideal for some applications (e.g. base-editing). In order to expand the set of curable vectors available for *Pseudomonas* species, we engineered synthetic control of replication for high-copy-number plasmids based on the *oriV*(pRO1600) replicon by introducing a conditional switch modulating the RepA protein.

Vector pSEVA448 was used as a template in these experiments, as it served as the backbone for constructing various pEdit plasmids (**Table 1**). Such plasmids harbor a hybrid of two origins of vegetative replication (i.e. pRO1600 and ColE1). The narrow-host-range *oriV*(ColE1) efficiently replicates in *E. coli* and *oriV*(pRO1600), obtained from a *P. aeruginosa* isolate, supports vector replication in *P. putida* and related species [37]. In order to manipulate replicon activity, we constructed a set of plasmids, termed pS44i8 (where '4i' indicates inducibility of the corresponding origin of replication), which bear an engineered *oriV*(pRO1600) module. This synthetic module was designed to contain a 3-*m*Bz–inducible XylS/*Pm* expression system to drive conditional expression of the *repA* gene that encodes the replication protein (**Fig. 3A**). In spite of its widespread use in bacterial genetics, the 5'-UTR region preceding *repA* has been poorly described (e.g. the presence and identity of promoters and Shine-Dalgarno sequences

remains virtually unknown), and we explored the native promoter and regulatory regions using *in silico* tools (i.e. BPROM from Softberry.com). Based on this analysis, we decided to test two designs, whereby the native *repA* is either left intact in front of the *Pm* promoter or completely replaced by the synthetic XylS/*Pm* module. These constructs would afford easy cloning and stable replication in *E. coli,* as the vectors still rely on the *oriV*(ColE) origin, whereas the plasmids would be rapidly and irreversibly lost in *Pseudomonas* in the absence of 3-*m*Bz. To test this setup *in vivo*, we set to compare the performance of the three plasmids under study: pSEVA448 (control vector), pS44i8GM (with a fully synthetic heterogeneous control of *repA* through the XylS/*Pm* system) and pS44i8GH-1 (bearing the native 5'-UTR region preceding *repA* and the *Pm* promoter). In order to facilitate the screening of bacterial colonies that had lost the plasmid, this set of vectors were additionally endowed with a *msfGFP* gene, encoding the monomeric superfolder green fluorescent protein. To confer constitutive expression of this reporter gene, we adapted the BG35/14b genetic element, containing the *msfGFP* gene under transcriptional control of the constitutive P_{14b} promoter together with a translational coupler (i.e. bicistronic design, spanning two Shine-Dalgarno sequences) [49]. These manipulations gave rise to conditionally replicating medium-copy pS44i8GM and high-copy pS44i8GH-1 plasmids (**Fig. 3A**).

P. putida KT2440 was transformed with either the control vector (i.e. pSEVA448) or the engineered plasmids, and the resulting recombinants were inoculated in a microtiter plate in LB medium containing 100 μg mL^{-1} Str at a starting OD_{600} = 0.05 in the presence of different inducer concentrations (0.5, 1 and 2 mM 3-m*Bz*). After 10 h of incubation at 30°C, cells reached the mid-exponential phase, and samples were collected from each well, diluted with PBS buffer to 1×10^3 cells per sample and stored at –20°C. Further analysis of gene expression and relative copy number quantification was performed by qPCR; plasmid copy numbers were calculated by estimating the *aadA* (Str^R) expression rates. We observed stable replication of all these plasmids in *P. putida*, with copy numbers that remained essentially within the same range regardless of the inducer concentration. Expectedly, no growth was registered in control experiments, where no 3-*m*Bz was added to the medium (data not shown). One of the engineered vectors, pS44i8GH-1, had a high-copy number (~32-38 copies per cell), similar to the original pSEVA448 vector (~35-42 copies per cell, **Fig. 3B**). These results correlated with previously reported data for SEVA vectors carrying *oriV*(pRO1600/ColE1) replicons [43,50]. The other engineered vector, plasmid pS44i8GM, in contrast, exhibited a medium-copy-number (~20-26 copies per cell, **Fig. 3B**). The detected variations in replication efficiency (hence, plasmid copy number) also resulted in different levels of

msfGFP production, exhibiting ~5-fold decrease in fluorescence for cells harboring pS44i8GM plasmids as compared to the msfGFP levels observed for *P. putida* KT2440/pS44i8GH-1 (data not shown). Hence, removing the native regulatory sequences and predicted promoter regions upstream of *repA* resulted in a tighter transcription control of the replication gene (**Fig. 3A**).

As the presence of fluorescent marker in vectors allows to perform direct screening of plasmid-bearing cells, we used fluorescence-activated cell sorting to analyze and quantify curing efficiency for the pS44i8GH-1 and pS44i8GM vectors. To this end, bacterial cultures of *P. putida* were grown for 16-20 h in 10 mL of LB medium upon inoculation at a starting OD_{600}~0.05 with different inducer concentrations (0, 0.5, 1 and 2 mM 3-m*Bz*). These cultures were washed and diluted with PBS buffer to a density of 1×10^3 cells per sample, followed by single-cell analysis by flow cytometry based on msfGFP fluorescence. We could observe a distribution of cells in the bacterial culture that was largely bimodal: a fraction of the cells positive for msfGFP fluorescence, and a population of cells negative for msfGFP signal, potentially indicating plasmid loss (**Fig. 3C**). When the recombinant cells were grown in the presence of 2 mM 3-*m*Bz, thereby sustaining vector replication, >90% of the bacterial population was recovered in the msfGFP$^+$ channel (**Fig. 3C**). In contrast, when cells carrying these vectors were cultivated in the absence of both antibiotic (Str) and inducer of replication (3-m*Bz*) for as little as 8 h, the efficiency of curing for plasmids pS44i8GH-1 (high-copy-number) and pS44i8GM (medium-copy-number) was ρ = 67% and 84%, respectively (**Fig. 3C**). In summary, the vectors described herein not only expand the set of curable plasmids that can be used in several manipulations, but they also provide an option of medium or high-copy-number depending on the cargo and application of interest. These results support exploiting vector curing as a strategy for transient activation of a plasmid-encoded functionality, followed by controllable vector loss and easy screening of desired phenotype(s) (**Fig. 3D**). This notion guided the next step in engineering a curable plasmid-based toolset for nearly PAM-less base-editing in *P. putida*.

The pAblo·pCasso toolset for unconstrained base-editing in Gram-negative bacteria

We constructed a pair of self-curing vectors, termed p**A**blo p**C**asso, for base-editing of **A**denine and **C**ytidine residues, respectively, in Gram-negative bacteria at the single-nucleotide resolution. To this end, and building on the data presented above, the curable vector pS44i8GH-1 (high-copy-number) was selected as the backbone for integrating the respective base-editor modules, placed under transcriptional

control of the *Pm* promoter. To avoid potential toxicity of the combination of the base-editor and a strong constitutive expression of *msfGFP* gene, we altered previously published [49] bicistronic design by removing BSD2 and keeping only one Shine-Dalgarno sequence and the constitutive P_{14b} promoter. This resulted in a plasmid pS448GH-2 without a translational coupler for *msfGFP* gene (**Table 1**). As the inducer (3-*m*Bz) is needed both for sustaining vector replication (i.e. *Pm*→*repA*) and expression of the base-editor construct (i.e. *Pm*→ABE or CBE), 3-*m*Bz was added to the culture media at 2 mM in all of the experiments described in this section. The physical map of the resulting pAblo pCasso vectors (~12 kbp) is presented in **Fig. 4A**, while the detailed structure of each base-editor is shown in **Fig. 1**.

The functionality of the pAblo pCasso vectors was demonstrated by creating a functional gene knockout (i.e. by integrating a *STOP* codon into the reading frame, with the pCasso plasmid), followed by restoring its function (i.e. reverting to the original genotype, with the pAblo plasmid). We adopted the nicotinic acid degradation pathway of *P. putida* KT2440 [24,51] as a testbed for the pAblo pCasso toolbox. To this end, we selected functional knockouts of the *nicX* gene, encoding a 2,5-dihydroxypyridine 5,6-dioxygenase, as an easy-to-screen phenotype. In particular, an interruption of the metabolic route at the level of 2,5-dihydroxypyridine leads to the accumulation of this dark green compound within and outside of the cells, which forms brown polymers upon exposure to oxygen and autoxidation. We designed spacers for the *nicX* gene endowed with non-canonical PAM motifs to target the Q7 codon (encoding a glutamine residue; **Fig. 4C-D** and **Table S1**, Supplementary Information) for both base-editors in an effort to demonstrate the ability of SpRY to increase accessibility to the target sequence.

As a first step, *P. putida* KT2440 was transformed with plasmid pCasso·*nicX*^{Q7} plasmid and the resulting strain was grown for 24 h in LB medium with 3-*m*Bz and Str. Upon platting the bacterial suspension onto LB medium agar containing 5 mM nicotinic acid and incubating the plates for an extra ~16 h, brown colonies accounted for most of the bacterial population (**Fig. 4C**). Around 30-40 individual colonies were picked from these plates, and the sequence of the *nicX* locus was inspected by PCR. According to this analysis, base-edited colonies represented ~40% of the entire bacterial population (**Fig. 4C**). Owing to the sequence of the region targeted, these manipulations led to a double C-to-T modification (i.e. 5'-**C**AA **C**TG-3'→5'-**T**AA **T**TG-3'). These observations indicate that the pCasso plasmid mediated efficient conversion of cytidine residues in *P. putida*. Next, the base-edited strain was isolated and streaked on LB agar plates (i.e. without any supplement) to promote plasmid curing. After a ~16 h incubation at 30°C,

non-fluorescent colonies were picked by placing the plates onto a blue light transilluminator (i.e. the absence of msfGFP fluorescence under blue light was taken as an indication of plasmid loss). In the next round of editing, we attempted to revert the functional knockout of *nicX* in *P. putida* to the original, wild-type genotype. Hence, the base-editing procedure was repeated by transforming vector-free *P. putida* cells (Δ*nicX*^{Q7}) with plasmid pAblo·*nicX*^{Q7}. The resulting cultures were incubated for 24 h in LB medium with 3-*m*Bz and Str, and the bacterial suspension was then plated onto LB medium agar added with nicotinic acid as explained above. Visual inspection of the plates indicated a wild-type phenotype for roughly half of the *P. putida* colonies; further analysis by PCR and sequencing of the amplicons indicated that both nucleotide substitutions were reverted to the original sequence with a ~30% efficiency (**Fig. 4D**). Moreover, after an 8-h cultivation in LB medium without any additives, virtually all the cells had lost plasmid pAblo·*nicX*^{Q7} (with ρ = 98%). Taken together, these results highlight the versatility of the CBE and ABE modules for engineering Gram-negative bacteria—demonstrated by a first-case example of site-directed mutation and reversal in the same strain. Moreover, the easily-curable vectors used for base-editing enable cycling of the genome modifications in a simple protocol that can be adapted to different purposes (including metabolic engineering and fundamental discovery of gene-to-function relationships) and amenable to automation [52]. This strategy eases complex strain engineering programs independently of homologous recombination and yields plasmid-free engineered cells. Based on these observations, in the next section we describe a general protocol for unconstrained base-editing in Gram-negative bacteria.

A step-by-step procedure for base-editing in *Pseudomonas* species

By applying the tools and procedures outlined in the previous sections, the entire protocol for one round of editing (starting with cloning of the plasmids and base-editing procedure) resulted in a 5-day workflow, schematically illustrated in **Fig. 5**. The specific steps needed for cytidine editing (using the pCasso vector) are detailed below as an example of implementation:

i. **Day 1** · Digest the pCasso vector with FastDigest *Eco*31I (or *Bsa*I) according to the manufacturer's recommendations. Purify the linearized plasmid after digestion by agarose gel purification of the digestion mixture *via* DNA electrophoresis. The fragment corresponding to the pCasso vector (~12 kbp) can be purified once in high quantities and stored as a concentrated stock to be used in

multiple applications. To boost ligation efficiency with the linearized vector, oligonucleotides can be phosphorylated using T4 polynucleotide kinase (PNK) or by chemical modification during oligonucleotide synthesis.

ii. Phosphorylation and annealing of the two spacer oligonucleotides (suspended at 100 μM) in a thermocycler. The mixture (10 μL in total) contains: 6 μL of water, 1 μL of each oligonucleotide suspension, 1 μL of T4 ligase buffer and 1 μL of T4 PNK (10 U μL^{-1}, Thermo Scientific). The reaction is incubated for 30 min at 37°C, 3 min at 95°C for phosphorylation and T4 PNK deactivation, followed by annealing cycles starting at 95°C and decreasing the temperature by 1°C in each cycle until 25°C.

iii. Ligation of the resulting spacer duplex obtained in (ii) into the linearized pCasso vector. The mixture of double-stranded DNA oligonucleotides should be diluted 1:200 with water. Then, a 10-μL reaction is prepared by mixing 5 μL of the diluted duplex supension, 1 μL (10 ng) of linearized pCasso vector, 1 μL of T4 ligase buffer, 1 μL of T4 DNA ligase (5 U μL^{-1}, Thermo Scientific) and 2 μL of water (which can be adjusted as needed to reach the final volume). The resulting mixture is incubated for 30 min at room temperature.

iv. Transformation of a 100-μL aliquot of chemically-competent *E. coli* DH5α cells with the 10-μL ligation mixture obtained in (iii). The bacterial suspension should be plated on LB agar plates supplemented with Str (100 μg mL^{-1}).

v. **Day 2** · The mini-prep–purified plasmid from two-three individual transformants is verified by DNA sequencing with primer 153 (**Table S1**, Supplementary Information).

vi. **Day 3** · Once the target-specific vectors are constructed and verified, they can be transformed in *Pseudomonas* for the target base-editing event. After transformation with the recombinant pCasso plasmid and recovery of the cells in LB medium for 2-4 h, a 10-μL aliquot of the bacterial suspension is inoculated in 10 mL of selective medium (LB medium added with 2 mM of 3-m*Bz* and 200 μg mL^{-1} Str) and grown overnight at 30°C. Optionally, the bacterial population could be subjected to passaging into fresh selective medium every 5 h to boost editing efficiency (by diluting the culture 1:100 in each passage). Aliquots of the bacterial suspension are plated onto selective medium.

vii. **Day 4** · Editing of the target locus should be verified at this stage by picking 10-15 individual colonies ($msfGFP^+$), PCR amplification of the target with appropriate oligonucleotides and DNA sequencing.

viii. **Day 5** · The last step of the sequence entails curing the base-editing plasmid. To this end, an individual colony (carrying the intended modification) should be streaked onto non-selective medium (LB medium without antibiotic or inducer). After a ~8-16 h incubation at 30°C, the cured (non-fluorescent) colonies can be peaked in a blue-light transilluminator and inoculated for the next round of editing or further strain characterization.

CONCLUSION

CRISPR-mediated nucleotide editing has only recently been established in bacteria but is already adapted for multiple purposes, both in fundamental discovery and practical applications [3]. While the PAM requirement of CRISPR systems provide sequence-specific adaptive immunity in bacteria, the strict nature of PAM recognition constrains CRISPR-Cas systems for genome editing applications [53]. The SpRY variant circumvent this limitation by relaxing the dependence of ^{Sp}Cas9 on a given PAM, extending targeting to sites with 5'-*NGN*-3' and 5'-*NAN*-3' PAMs—as well as other sites, albeit with a reduced recognition efficiency. In this work, we have designed and implemented an SpRY-based, plasmid-borne toolbox to break a PAM restriction barrier during base-editing of *Pseudomonas* genomes. We used this nearly PAM-less ^{Sp}Cas9 variant to adapt two kinds of base-editors (i.e. ABE and CBE) to enable high-resolution substitutions of virtually any nucleotide in the genome. Here, we demonstrated high-efficiency base-editing in Gram-negative bacteria with an evolved ABEmax variant [36], so far restricted to genome engineering of mammalian cells. Moreover, its purposeful combination with the PAM-unrestricted SpRY protein [8] enabled easy editing of DNA sequences, securing a promising position in the synthetic biology toolbox for bacterial engineering. Furthermore, we implemented a fast and efficient approach for plasmid curing, based on the conditional replication of the parent vectors. These vectors can be equipped with any cargo of choice, which could be eliminated from the strain upon the absence of the inducer in the medium. By combining this system with the PAM-promiscuous base-editor variants, we constructed the pAblo·pCasso toolset, which demonstrates programmed nucleotide substitution, followed by the controlled plasmid curing from the modified strain. In conclusion, the bacterial genome engineering approach presented here enables robust constrain-less DNA modification and paves the way for multiple CRISPR-Cas applications in other bacterial systems [54].

Data Availability

The data underlying this article are available in the article and in its supplementary material. All plasmids and data generated in this study are available on request. Requests for materials should be made to the corresponding author.

Authors' Contributions

E.K.: Conceptualization, Investigation, Data curation, Methodology, Validation, Visualization, Writing – original draft. **Z.S.N.:** Investigation, Data curation, Methodology. **P.I.N:** Conceptualization, Project administration, Supervision, Resources, Data curation, Funding acquisition, Writing – review & editing.

Acknowledgements

We are thankful to Manuel Nieto-Domínguez for the help with base-editing experiments and imaging, Daria Sergeeva for the technical assistance with qPCR experiments and Mari Rodriguez de Evgrafov for the support with the flow cytometry set-up and analysis. The generous financial support from The Novo Nordisk Foundation through grants NNF20CC0035580, *LiFe* (NNF18OC0034818) and *TARGET* (NNF21OC0067996), and the European Union's Horizon 2020 Research and Innovation Programme under grant agreement No. 814418 (*SinFonia*) to P.I.N. is gratefully acknowledged. E.K. was supported by the Novo Nordisk Foundation (grant NNF17CC0026768) as part of the Copenhagen Bioscience Ph.D. Programme. The authors declare that there are no competing interests associated with the contents of this article.

References

1. Wang JY, Pausch P, Doudna JA: **Structural biology of CRISPR-Cas immunity and genome editing enzymes**. *Nat. Rev. Microbiol.* 2022, **20**:641-656.
2. Wang JY, Doudna JA: **CRISPR technology: A decade of genome editing is only the beginning**. *Science* 2023, **379**:eadd8643.

3. Cho S, Shin J, Cho BK: **Applications of CRISPR/Cas system to bacterial metabolic engineering**. *Int. J. Mol. Sci.* 2018, **19**:E1089.

4. Zhao D, Zhu X, Zhou H, Sun N, Wang T, Bi C, Zhang X: **CRISPR-based metabolic pathway engineering**. *Metab. Eng.* 2021, **63**:148-159.

5. Anzalone AV, Koblan LW, Liu DR: **Genome editing with CRISPR-Cas nucleases, base editors, transposases and prime editors**. *Nat. Biotechnol.* 2020, **38**:824-844.

6. Nishida K, Kondo A: **CRISPR-derived genome editing technologies for metabolic engineering**. *Metab. Eng.* 2020, **63**:141-147.

7. Sun J, Lu LB, Liang TX, Yang LR, Wu JP: **CRISPR-assisted multiplex base editing system in *Pseudomonas putida* KT2440**. *Front. Bioeng. Biotechnol.* 2020, **8**:905.

8. Walton RT, Christie KA, Whittaker MN, Kleinstiver BP: **Unconstrained genome targeting with near-PAMless engineered CRISPR-Cas9 variants**. *Science* 2020, **368**:290-296.

9. Komor AC, Kim YB, Packer MS, Zuris JA, Liu DR: **Programmable editing of a target base in genomic DNA without double-stranded DNA cleavage**. *Nature* 2016, **533**:420-424.

10. Komor AC, Zhao KT, Packer MS, Gaudelli NM, Waterbury AL, Koblan LW, Kim YB, Badran AH, Liu DR: **Improved base excision repair inhibition and bacteriophage Mu Gam protein yields C:G-to-T:A base editors with higher efficiency and product purity**. *Sci. Adv.* 2017, **3**:eaao4774.

11. Gaudelli NM, Komor AC, Rees HA, Packer MS, Badran AH, Bryson DI, Liu DR: **Programmable base editing of A*T to G*C in genomic DNA without DNA cleavage**. *Nature* 2017, **551**:464-471.

12. Sapranauskas R, Gasiunas G, Fremaux C, Barrangou R, Horvath P, Siksnys V: **The *Streptococcus thermophilus* CRISPR/Cas system provides immunity in *Escherichia coli***. *Nucleic Acids Res.* 2011, **39**:9275-9282.

13. Jiang W, Bikard D, Cox D, Zhang F, Marraffini LA: **RNA-guided editing of bacterial genomes using CRISPR-Cas systems**. *Nat. Biotechnol.* 2013, **31**:233-239.

14. Gasiunas G, Barrangou R, Horvath P, Siksnys V: **Cas9-crRNA ribonucleoprotein complex mediates specific DNA cleavage for adaptive immunity in bacteria**. *Proc. Natl. Acad. Sci. USA* 2012, **109**:E2579-2586.

15. Shelake RM, Pramanik D, Kim JY: ***In vivo* rapid investigation of CRISPR-based base editing components in *Escherichia coli* (IRI-CCE): A platform for evaluating base editing tools and their components**. *Int. J. Mol. Sci.* 2022, **23**:1145.

16. Schultenkämper K, Brito LF, Wendisch VF: **Impact of CRISPR interference on strain development in biotechnology**. *Biotechnol. Appl. Biochem.* 2020, **67**:7-21.
17. Weimer A, Kohlstedt M, Volke DC, Nikel PI, Wittmann C: **Industrial biotechnology of *Pseudomonas putida*: Advances and prospects**. *Appl. Microbiol. Biotechnol.* 2020, **104**:7745–7766.
18. Volke DC, Calero P, Nikel PI: ***Pseudomonas putida***. *Trends Microbiol.* 2020, **28**:512-513.
19. Brinkman FSL, Winsor GL, Done RE, Filloux A, Francis VI, Goldberg JB, Greenberg EP, Han K, Hancock REW, Haney CH, et al.: **The *Pseudomonas aeruginosa* whole genome sequence: A 20th anniversary celebration**. *Adv. Microb. Physiol.* 2021, **79**:25-88.
20. Volke DC, Nikel PI: **Getting bacteria in shape: Synthetic morphology approaches for the design of efficient microbial cell factories**. *Adv. Biosyst.* 2018, **2**:1800111.
21. Kozaeva E, Volkova S, Matos MRA, Mezzina MP, Wulff T, Volke DC, Nielsen LK, Nikel PI: **Model-guided dynamic control of essential metabolic nodes boosts acetyl-coenzyme A–dependent bioproduction in rewired *Pseudomonas putida***. *Metab. Eng.* 2021, **67**:373-386.
22. Martínez-García E, de Lorenzo V: ***Pseudomonas putida* in the quest of programmable chemistry**. *Curr. Opin. Biotechnol.* 2019, **59**:111-121.
23. Abdullah A, Wang P, Han T, Liu W, Ren W, Wu Y, Xiao Y: **Adenine base editing system for *Pseudomonas* and prediction workflow for protein dysfunction *via* ABE**. *ACS Synth. Biol.* 2022, **11**:1650-1657.
24. Volke DC, Martino RA, Kozaeva E, Smania AM, Nikel PI: **Modular (de)construction of complex bacterial phenotypes by CRISPR/nCas9-assisted, multiplex cytidine base-editing**. *Nat. Commun.* 2022, **13**:3026.
25. Yue SJ, Huang P, Li S, Cai YY, Wang W, Zhang XH, Nikel PI, Hu HB: **Developing a CRISPR-assisted base-editing system for genome engineering of *Pseudomonas chlororaphis***. *Microb. Biotechnol.* 2022, **15**:2324-2336.
26. Cavaleiro AM, Kim SH, Seppälä S, Nielsen MT, Nørholm MH: **Accurate DNA assembly and genome engineering with optimized uracil excision cloning**. *ACS Synth. Biol.* 2015, **4**:1042-1046.
27. Genee HJ, Bonde MT, Bagger FO, Jespersen JB, Sommer MOA, Wernersson R, Olsen LR: **Software-supported *USER* cloning strategies for site-directed mutagenesis and DNA assembly**. *ACS Synth. Biol.* 2015, **4**:342-349.

28. Batianis C, Kozaeva E, Damalas SG, Martín-Pascual M, Volke DC, Nikel PI, Martins dos Santos VAP: **An expanded CRISPRi toolbox for tunable control of gene expression in *Pseudomonas putida***. *Microb. Biotechnol.* 2020, **13**:368-385.

29. Fernández-Cabezón L, Rosich i Bosch B, Kozaeva E, Gurdo N, Nikel PI: **Dynamic flux regulation for high-titer anthranilate production by plasmid-free, conditionally-auxotrophic strains of *Pseudomonas putida***. *Metab. Eng.* 2022, **73**:11-25.

30. Livak KJ, Schmittgen TD: **Analysis of relative gene expression data using real-time quantitative PCR and the 2^{-DDCT} method**. *Methods* 2001, **25**:402-408.

31. Nikel PI, Benedetti I, Wirth NT, de Lorenzo V, Calles B: **Standardization of regulatory nodes for engineering heterologous gene expression: a feasibility study**. *Microb. Biotechnol.* 2022, **15**:2250-2265.

32. Hahne F, LeMeur N, Brinkman RR, Ellis B, Haaland P, Sarkar D, Spidlen J, Strain E, Gentleman R: **FlowCore: a Bioconductor package for high throughput flow cytometry**. *BMC Bioinformatics* 2009, **10**:106.

33. Liang F, Zhang Y, Li L, Yang Y, Fei JF, Liu Y, Qin W: **SpG and SpRY variants expand the CRISPR toolbox for genome editing in zebrafish**. *Nat. Commun.* 2022, **13**:3421.

34. Ren Q, Sretenovic S, Liu S, Tang X, Huang L, He Y, Liu L, Guo Y, Zhong Z, Liu G, et al.: **PAM-less plant genome editing using a CRISPR-SpRY toolbox**. *Nat. Plants* 2021, **7**:25-33.

35. Evans BA, Bernstein DA: **SpRY Cas9 can utilize a variety of protospacer adjacent motif site sequences to edit the *Candida albicans* genome**. *mSphere* 2021, **6**.

36. Gaudelli NM, Lam DK, Rees HA, Sola-Esteves NM, Barrera LA, Born DA, Edwards A, Gehrke JM, Lee SJ, Liquori AJ, et al.: **Directed evolution of adenine base editors with increased activity and therapeutic application**. *Nat. Biotechnol.* 2020, **38**:892-900.

37. Silva-Rocha R, Martínez-García E, Calles B, Chavarría M, Arce-Rodríguez A, de las Heras A, Páez-Espino AD, Durante-Rodríguez G, Kim J, Nikel PI, et al.: **The Standard European Vector Architecture (SEVA): a coherent platform for the analysis and deployment of complex prokaryotic phenotypes**. *Nucleic Acids Res.* 2013, **41**:D666-D675.

38. Martínez-García E, Fraile S, Algar E, Aparicio T, Velázquez E, Calles B, Tas H, Blázquez B, Martín B, Prieto C, et al.: **SEVA 4.0: An update of the Standard European Vector Architecture database for advanced analysis and programming of bacterial phenotypes**. *Nucleic Acids Res.* 2023, **51**:D1558-D1567.

39. Ladunga I: **Finding similar nucleotide sequences using network BLAST searches**. *Curr. Protoc. Bioinformatics* 2017, **58**:3.3.1-3.3.25.

40. Kunne T, Swarts DC, Brouns SJ: **Planting the seed: target recognition of short guide RNAs**. *Trends Microbiol.* 2014, **22**:74-83.

41. Wiedenheft B, van Duijn E, Bultema JB, Waghmare SP, Zhou K, Barendregt A, Westphal W, Heck AJ, Boekema EJ, Dickman MJ, et al.: **RNA-guided complex from a bacterial immune system enhances target recognition through seed sequence interactions**. *Proc. Natl. Acad. Sci. USA* 2011, **108**:10092-10097.

42. Tong Y, Whitford CM, Blin K, Jørgensen TS, Weber T, Lee SY: **CRISPR-Cas9, CRISPRi and CRISPR-BEST-mediated genetic manipulation in streptomycetes**. *Nat. Protoc.* 2020, **15**:2470-2502.

43. Jahn M, Vorpahl C, Hübschmann T, Harms H, Müller S: **Copy number variability of expression plasmids determined by cell sorting and droplet digital PCR**. *Microb. Cell Fact.* 2016, **15**:211.

44. Ma J, Campbell A, Karlin S: **Correlations between Shine-Dalgarno sequences and gene features such as predicted expression levels and operon structures**. *J. Bacteriol.* 2002, **184**:5733-5745.

45. Cao X, Slavoff SA: **Non-AUG start codons: Expanding and regulating the small and alternative ORFeome**. *Exp. Cell Res.* 2020, **391**:111973.

46. Belinky F, Rogozin IB, Koonin EV: **Selection on start codons in prokaryotes and potential compensatory nucleotide substitutions**. *Sci. Rep.* 2017, **7**:12422.

47. Buckner MMC, Ciusa ML, Piddock LJV: **Strategies to combat antimicrobial resistance: anti-plasmid and plasmid curing**. *FEMS Microbiol. Rev.* 2018, **42**:781-804.

48. Volke DC, Friis L, Wirth NT, Turlin J, Nikel PI: **Synthetic control of plasmid replication enables target- and self-curing of vectors and expedites genome engineering of *Pseudomonas putida***. *Metab. Eng. Commun.* 2020, **10**:e00126.

49. Zobel S, Benedetti I, Eisenbach L, de Lorenzo V, Wierckx NJP, Blank LM: **Tn7-Based device for calibrated heterologous gene expression in *Pseudomonas putida***. *ACS Synth. Biol.* 2015, **4**:1341-1351.

50. Cook TB, Rand JM, Nurani W, Courtney DK, Liu SA, Pfleger BF: **Genetic tools for reliable gene expression and recombineering in *Pseudomonas putida***. *J. Ind. Microbiol. Biotechnol.* 2018, **45**:517-527.

51. Wirth NT, Kozaeva E, Nikel PI: **Accelerated genome engineering of *Pseudomonas putida* by I-*Sce*I—mediated recombination and CRISPR-Cas9 counterselection**. *Microb. Biotechnol.* 2020, **13**:233-249.

52. Gurdo N, Volke DC, Nikel PI: **Merging automation and fundamental discovery into the design–build–test–learn cycle of nontraditional microbes**. *Trends Biotechnol.* 2022, **40**:1148-1159.

53. Adli M: **The CRISPR tool kit for genome editing and beyond**. *Nat. Commun.* 2018, **9**:1911.

54. Liu Z, Dong H, Cui Y, Cong L, Zhang D: **Application of different types of CRISPR/Cas-based systems in bacteria**. *Microb. Cell Fact.* 2020, **19**:172.

55. Hanahan D, Meselson M: **Plasmid screening at high colony density**. *Methods Enzymol.* 1983, **100**:333-342.

56. Worsey MJ, Williams PA: **Metabolism of toluene and xylenes by *Pseudomonas putida* (*arvilla*) mt-2: evidence for a new function of the TOL plasmid**. *J. Bacteriol.* 1975, **124**:7-13.

57. Bagdasarian M, Lurz R, Rückert B, Franklin FCH, Bagdasarian MM, Frey J, Timmis KN: **Specific purpose plasmid cloning vectors. II. Broad host range, high copy number, RSF1010-derived vectors, and a host-vector system for gene cloning in *Pseudomonas***. *Gene* 1981, **16**:237-247.

TABLES

Table 1. Bacterial strains and plasmids used in this study.

Bacterial strain	Relevant characteristics[a]	Reference or source
Escherichia coli		
DH5α λ*pir*	Cloning host; F^- λ^- *endA1 glnX44*(AS) *thiE1 recA1 relA1 spoT1 gyrA96*(Nal^R) *rfbC1 deoR nupG* Φ80(*lacZ*Δ*M15*) Δ(*argF-lac*)*U169 hsdR17*(r_K^- m_K^+), λ*pir* lysogen	[55]
Pseudomonas putida		
KT2440	Wild-type strain, derived from *P. putida* mt-2 [56] cured of the catabolic TOL plasmid pWW0	[57]
KT·YFP·mCherry	Derivative of strain KT2440 carrying a P_{EM7}→*mCherry* and a P_{EM7}→*yfp* cassette integrated in the Tn*7* locus, Km^R	[28]
Plasmid	**Relevant characteristics[a]**	**Reference or source**
pMCRi	Plasmid for CRISPRi; *oriV*(pRO1600/ColE1), *xylS* (cured of *Bsa*I-sites), *Pm*→^{Sp}*dCas9*, P_{EM7}→sgRNA; Sm^R/Sp^R	[28]
pEditA	Plasmid for adenine base editing; *oriV*(pRO1600/ColE1), *xylS* (cured of *Bsa*I-sites), *Pm*→ ABE:^{Sp}*nCas9*, P_{EM7}→non-specific sgRNA; Sm^R/Sp^R	This work
pEditA-RY	Plasmid for adenine base editing; *oriV*(pRO1600/ColE1), *xylS* (cured of *Bsa*I-sites), *Pm*→ABE:*SpRY*, P_{EM7}→non-specific sgRNA; Sm^R/Sp^R	This work
pEditC	Plasmid for cytidine base editing; *oriV*(pRO1600/ColE1), *xylS* (cured of *Bsa*I-sites), *Pm*→CBE:^{Sp}*nCas9*, P_{EM7}→non-specific sgRNA; Sm^R/Sp^R	This work
pEditC-RY	Plasmid for cytidine base editing; *oriV*(pRO1600/ColE1), *xylS* (cured of *Bsa*I-sites), *Pm*→CBE:*SpRY*, P_{EM7}→non-specific sgRNA; Sm^R/Sp^R	This work
pS2313	Standard expression vector; *oriV*(pBBR1), P_{EM7}; Km^R	[51]
pS2313·*mCherry*	Reporter plasmid; *oriV*(pBBR1), P_{EM7}→*mCherry*; Km^R	This work

pEditC·*mCherry*^{Q47}	Plasmid for cytidine editing of the *mCherry* Q47 codon; *oriV*(pRO1600/ColE1), *xylS* (cured of *Bsa*I-sites), *Pm*→CBE:^{Sp}*nCas9*, P_{EM7}→*mCherry*^{Q47}-specific sgRNA; Sm^R/Sp^R	This work
pEditC·*mCherry*^{W64}	Plasmid for cytidine editing of the *mCherry* W63 codon; *oriV*(pRO1600/ColE1), *xylS* (cured of *Bsa*I-sites), *Pm*→CBE:^{Sp}*nCas9*, P_{EM7}→*mCherry*^{W64}-specific sgRNA; Sm^R/Sp^R	This work
pEditC-RY·*mCherry*^{Q47}	Plasmid for cytidine editing of the *mCherry* Q47 codon; *oriV*(pRO1600/ColE1), *xylS* (cured of *Bsa*I-sites), *Pm*→CBE:*SpRY*, P_{EM7}→*mCherry* ^{Q47}-specific sgRNA; Sm^R/Sp^R	This work
pEditC-RY·*mCherry*^{W64}	Plasmid for cytidine editing of the *mCherry* W63 codon; *oriV*(pRO1600/ColE1), *xylS* (cured of *Bsa*I-sites), *Pm*→CBE:*SpRY*, P_{EM7}→*mCherry*^{W64}-specific sgRNA; Sm^R/Sp^R	This work
pEditA·*mCherry*^{M1}-1	Plasmid for adenine base editing of the *mCherry* M1 codon, PAM1; *oriV*(pRO1600/ColE1), *xylS* (cured of *Bsa*I-sites), *Pm*→ABE:^{Sp}*nCas9*, P_{EM7}→ *mCherry*^{START}-specific sgRNA1; Sm^R/Sp^R	This work
pEditA·*mCherry*^{M1}-2	Plasmid for adenine base editing of the *mCherry* M1 codon, PAM2; *oriV*(pRO1600/ColE1), *xylS* (cured of *Bsa*I-sites), *Pm*→ABE:^{Sp}*nCas9*, P_{EM7}→*mCherry*^{START}-specific sgRNA2; Sm^R/Sp^R	This work
pEditA·*mCherry*^{M1}-3	Plasmid for adenine base editing of the *mCherry* M1 codon, PAM3; *oriV*(pRO1600/ColE1), *xylS* (cured of *Bsa*I-sites), *Pm*→ABE:^{Sp}*nCas9*, P_{EM7}→*mCherry*^{START}-specific sgRNA3; Sm^R/Sp^R	This work
pEditA-RY·*mCherry*^{M1}-1	Plasmid for adenine base editing of the *mCherry* M1 codon, PAM1; *oriV*(pRO1600/ColE1), *xylS* (cured of *Bsa*I-sites), *Pm*→ABE:*SpRY*, P_{EM7}→*mCherry*^{START}-specific sgRNA1; Sm^R/Sp^R	This work
pEditA-RY·*mCherry*^{M1}-2	Plasmid for adenine base editing of the *mCherry* M1 codon, PAM2; *oriV*(pRO1600/ColE1), *xylS* (cured of *Bsa*I-sites), *Pm*→ABE:*SpRY*, P_{EM7}→*mCherry*^{START}-specific sgRNA2; Sm^R/Sp^R	This work

pEditA-RY·*mCherry*^{M1}-3	Plasmid for adenine base editing of the *mCherry* M1 codon, PAM3; *oriV*(pRO1600/ColE1), *xylS* (cured of *Bsa*I-sites), *Pm*→ABE:*SpRY*, P_{EM7}→*mCherry*^{START}-specific sgRNA3; Sm^R/Sp^R	This work
pSEVA448	Standard expression vector; *oriV*(pRO1600/ColE1), *xylS*, *Pm*; Sm^R/Sp^R	[37]
pS44i8GH-1	Conditionally-replicating derivative of vector pSEVA448, high-copy-number; *oriV*(pRO1600/ColE1), *xylS* (cured of *Bsa*I-sites), *Pm*→*repA*, P_{14b} *with a translational BCD2 coupler from BG35* [49]→*msfGFP*; Sm^R/Sp^R	This work
pS44i8GH-2	Conditionally-replicating derivative of vector pSEVA448, high-copy-number; *oriV*(pRO1600/ColE1), *xylS* (cured of *Bsa*I-sites), *Pm*→*repA*, P_{14b}→*msfGFP*; Sm^R/Sp^R	This work
pS44i8GM	Conditionally-replicating derivative of vector pSEVA448, medium-copy-number; *oriV*(pRO1600/ColE1), *xylS* (cured of *Bsa*I-sites), *Pm*→*repA*, P_{14b} *with a translational BCD2 coupler from BG35* [49]→*msfGFP*; Sm^R/Sp^R	This work
pAblo	Conditionally-replicating plasmid for adenine base editing based on pS44i8GH-2; *oriV*(pRO1600/ColE1), *xylS* (cured of *Bsa*I-sites), *Pm*→*repA*, P_{14b}→*msfGFP*; *Pm*→ ABE:*SpRY*, P_{EM7}→non-specific sgRNA; Sm^R/Sp^R	This work
pCasso	Conditionally-replicating plasmid for cytidine base editing based on pS44i8GH-2; *oriV*(pRO1600/ColE1), *xylS* (cured of *Bsa*I-sites), *Pm*→*repA*, P_{14b}→*msfGFP*; *Pm*→CBE:*SpRY*, P_{EM7}→non-specific sgRNA; Sm^R/Sp^R	This work
pAblo·*nicX*^{Q7}	Conditionally-replicating plasmid for adenine base editing of codon Q7 in *nicX*; *oriV*(pRO1600/ColE1), *xylS* (cured of *Bsa*I-sites), *Pm*→*repA*, P_{14b}→*msfGFP*; *Pm*→ ABE:*SpRY*, P_{EM7}→*nicX*^{Q7}-specific sgRNA; Sm^R/Sp^R	This work
pCasso·*nicX*^{Q7}	Conditionally-replicating plasmid for cytidine base editing of codon Q7 in *nicX*; *oriV*(pRO1600/ColE1), *xylS* (cured of *Bsa*I-sites), *Pm*→*repA*, P_{14b}→*msfGFP*; *Pm*→ CBE:*SpRY*, P_{EM7}→*nicX*^{Q7}-specific sgRNA; Sm^R/Sp^R	This work

1 [a] Antibiotic markers: Km, kanamycin; Sm, streptomycin; and Sp, spectinomycin.

FIGURES

Figure 1. Mechanistic features of the CRISPR/^{Sp}nCas9 base-editors in this study and their applications for bacterial genome editing.

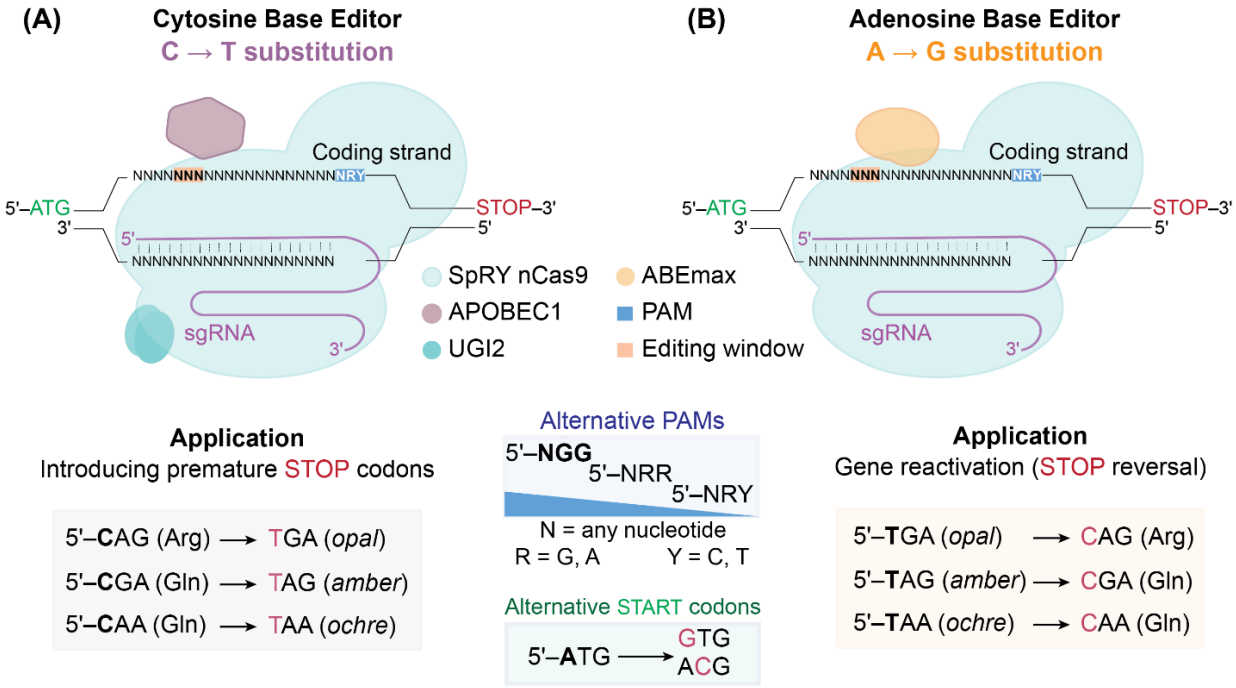

(A) Cytidine base-editor. A fusion of SpRY to APOBEC1 (apolipoprotein B mRNA editing enzyme) and a duplex UGI (uracil DNA glycosylase inhibitor) allows for cytidine-to-thymine substitutions. Such editing tool can be useful for integrating premature *STOP* codon(s) into the reading frame of gene(s) of interest (*opal*, *amber* or *ochre* codons), thus resulting in a functional knock-out. **(B)** Adenine base-editor. In this case, the SpRY nCas9 protein is fused with an evolved variant of the adenine deaminase enzyme (ABEmax) that enables adenine-to-guanine substitutions. Application examples of the tool include restoring gene functionality by re-editing premature *STOP* codon(s) back to the wild-type sequence or introduction of alternative *START* codons. Both base-editors have a relaxed specificity for the cognate PAM (protospacer adjacent motif) as indicated in the diagram.

Figure 2. Calibrating cytidine and adenine base-editing in *P. putida*.

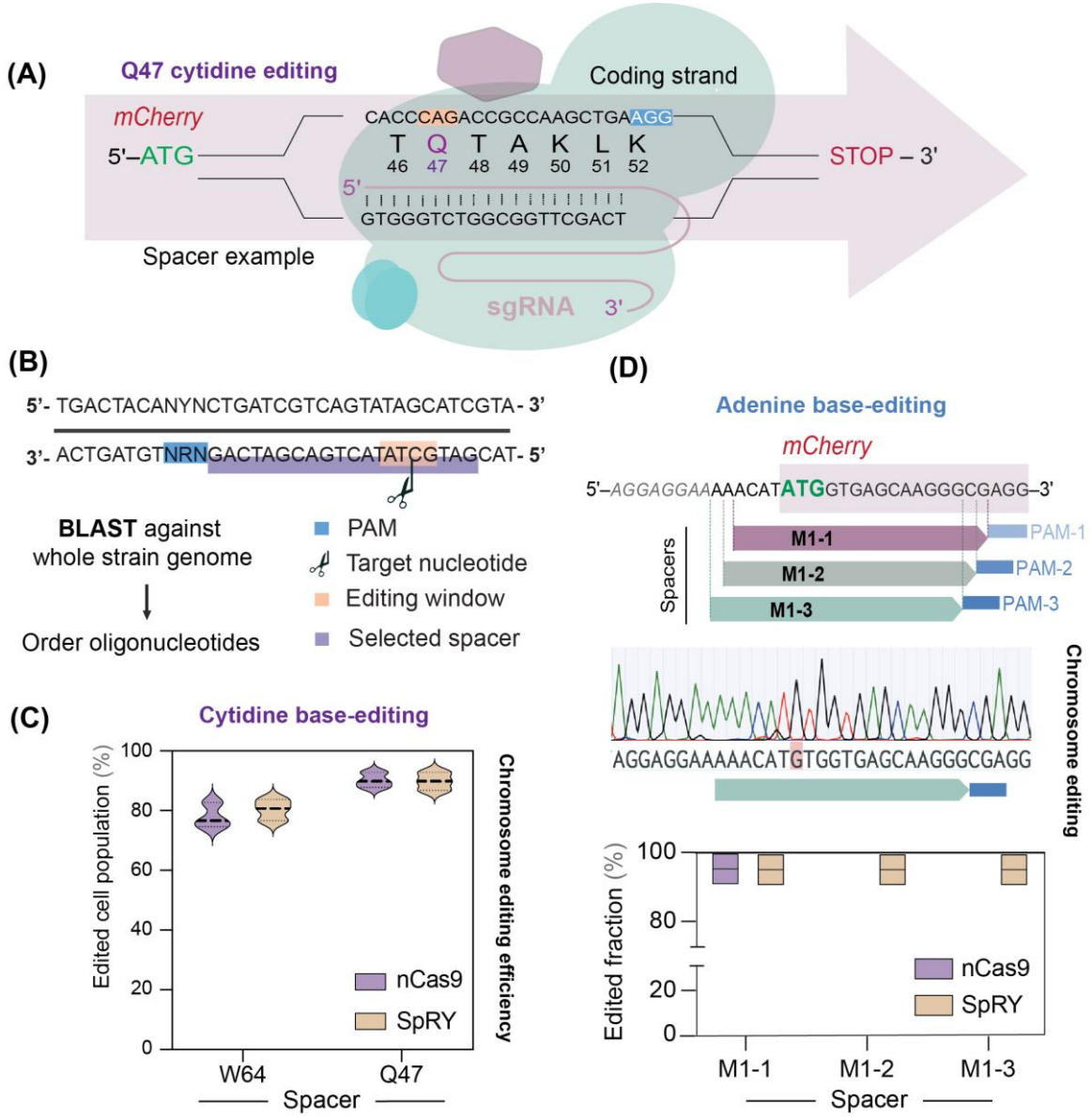

Cytidine and adenine base-editing in *P. putida*, targeting the *mCherry* gene (either integrated as a single-copy module into the chromosome or expressed from plasmid pS2313·*mCherry*), compared through the implementation of either ^{Sp}nCas9 or the evolved SpRY variant with spacers displaying classical or non-canonical PAM motifs. **(A)** Schematic representation of an example spacer to edit the cytidine residue within the Q47 codon of *mCherry*; this substitution would result in a premature *STOP* codon. **(B)** Design of target spacers. A PAM sequence (5'-*NRN*-3', where *N* represents any nucleotide and R is either an adenine or a guanine residue) is chosen within the gene of interest, and downstream of the selected target nucleotide. The selected spacer in this case is 20-bp long, and the sequence should be validated *via* BLAST against the whole genome to minimize off-target effects. In the example shown herein, the

optimal editing window is highlighted in orange. **(C)** Cytidine base-editing in *P. putida*. Editing efficiency was calculated after 24 h of treatment based on a fluorescence assay and verified by flow cytometry and DNA sequencing of individual clones. The wild-type *P. putida* KT2440 strain (transformed with plasmid pS2313·*mCherry*) or strain KT·YFP·mCherry (harboring *mCherry* integrated into the Tn7 locus of the bacterial chromosome) were used as positive controls in these experiments; strain KT2440 was used as a negative control. Different spacers were tested to compare the base-editing performance of the canonical ^{Sp}nCas9 or the evolved SpRY variant. **(D)** Adenine base-editing in *P. putida*. The diagram shows a schematic representation of the spacers tested to edit the first adenine residue within the *START* codon. The M1-1 spacer encodes the classical 5'-*N*GG-3' PAM, whereas M1-2 and M1-3 display the alternative, non-canonical 5'-*N*RG-3' and 5'-*N*GR-3' PAMs, respectively. Editing efficiency was calculated after 24 h of treatment as indicated for the experiments in panel **(C)**. These experiments were independently repeated three times, and the colonies were pooled for the analysis.

Figure 3. Engineering conditional plasmid replication for *P. putida* using a high-copy-number vector of the SEVA framework.

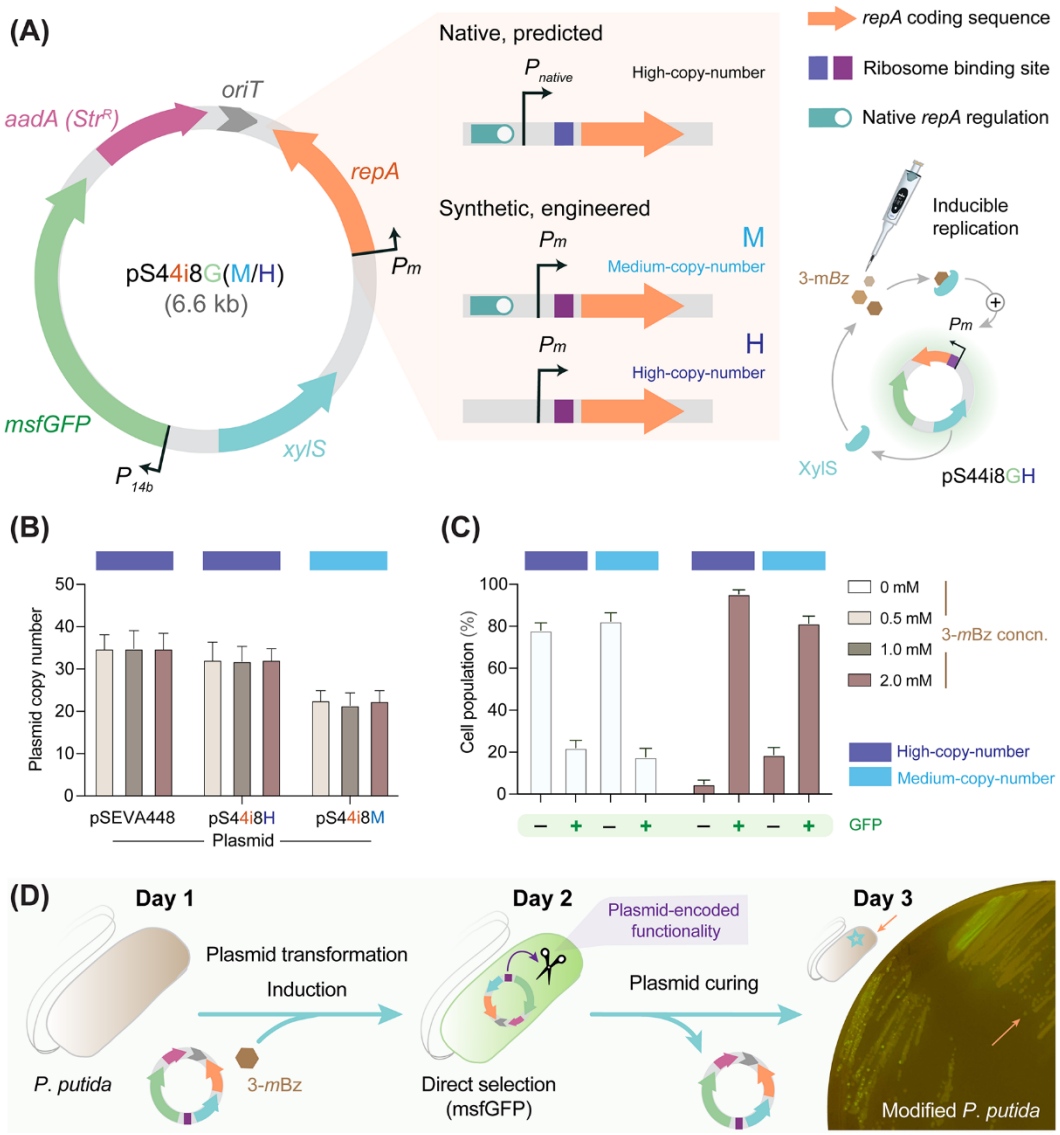

(A) Representation of the structure and functional modules in vector pS44i8G and derivatives. Integration of a synthetic RBS and a XylS/*Pm* module to replace the native transcription initiation regulation of *repA* in *oriV*(RO1600) resulted in high- and medium-copy-number plasmid variants. **(B)** Vector stability analysis by relative copy number quantification of vectors pSEVA448 (control), pS44i8GH-1 (high-copy-number) and pS44i8GM (medium-copy-number) in *P. putida* cells after 10 h of growth (mid-exponential phase) with different concentrations of the inducer (0.5, 1 and 2 mM 3-m*Bz*). Plasmid copy number was calculated by normalizing expression rates measured using qPCR of the plasmid-borne *aadA* gene (Str^R) and the chromosomal *rpoB* gene [29], and compared with the reference plasmid (pSEVA448 [38,43]). **(C)** Curing efficiency of vectors pS44i8GH and pS44i8GM upon using different concentrations of inducer

that sustains plasmid replication. *P. putida* cells carrying either plasmid were grown for 16 h in LB medium with (0.5, 1 or 2 mM) and without 3-m*Bz*. The culture was diluted with PBS buffer to adjust the cell density to 1×10^3 cells per sample and analyzed by flow cytometry based on msfGFP fluorescence. Negative (–) cell populations did not display any detectable msfGFP signal (plasmid-free cells); the positive (+) population, in contrast, had different levels of msfGFP as indicated (plasmid-baring cells). **(D)** Schematic representation of the selection and plasmid curing approach. The replication of the synthetic *oriV* construct is supported by the presence of 3-m*Bz*. Cells transformed with the respective vector were grown with 1 mM 3-mBz. On day 2 of the protocol, cells containing msfGFP are selected, and strain manipulation is done with addition of inducer to sustain vector replication. On day 3, cells are grown in selection-free medium (i.e. no antibiotic or inducer) and directly plated onto LB medium *via* dilution-streak to isolate plasmid-free ($msfGFP^-$) colonies. Note that conditional-replication plasmids carry essentially any potential functionality that may be required transiently for genome editing.

Figure 4. Base-editing strategy pAblo pCasso consisting of vectors with conditional plasmid replication.

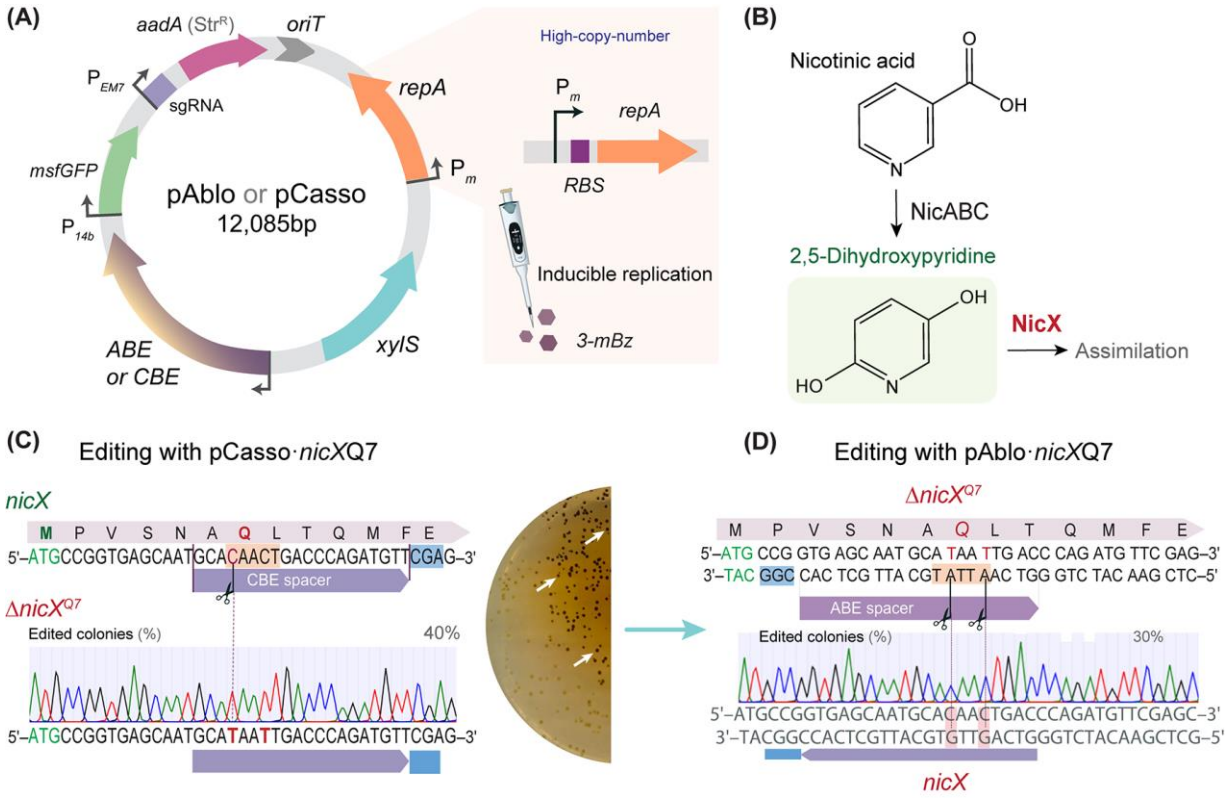

(A) Schematic representation of the constructed plasmids and their functional elements. Abbreviations are as follows: ABE, adenine base-editor; CBE, cytidine base-editor, msfGFP, monomeric superfolder green fluorescent protein; and sgRNA, single guide RNA. The inducible replication module ($P_m \rightarrow repA$) is also represented. **(B)** Nicotinic acid degradation pathway in *P. putida* [24,51]. Functional knock-out of the gene encoding NicX leads to 2,5-dihydroxypyridine accumulation and a brown-colony phenotype. **(C)** Example of base-editing of the *nicX* gene, encoding 2,5-dihydroxypyridine dioxygenase, with plasmid pCasso·*nicX*^{Q7} in *P. putida* KT2440. The Q7 glutamine codon (5'-CAA-3') was targeted to incorporate a premature *STOP* codon (5'-TAA-3') in the reading frame. The functional gene knockout was confirmed by the dark-colony phenotype (indicative of the accumulation of 2,5-dihydroxypyridine), as illustrated in the plate (LB medium containing 5 mM nicotinic acid) photograph. **(D)** Example of base-editing of the *nicX* gene with plasmid pAblo·*nicX*^{Q7} to restore the wild-type phenotype. Gene sequence was reverted to original with ~30% efficiency for two editing events (5'-TAATTG-3'→5'-CAACTG-3') and confirmed by sequencing of at least 25 single picked colonies.

Figure 5. Workflow for base-editing in *Pseudomonas*.

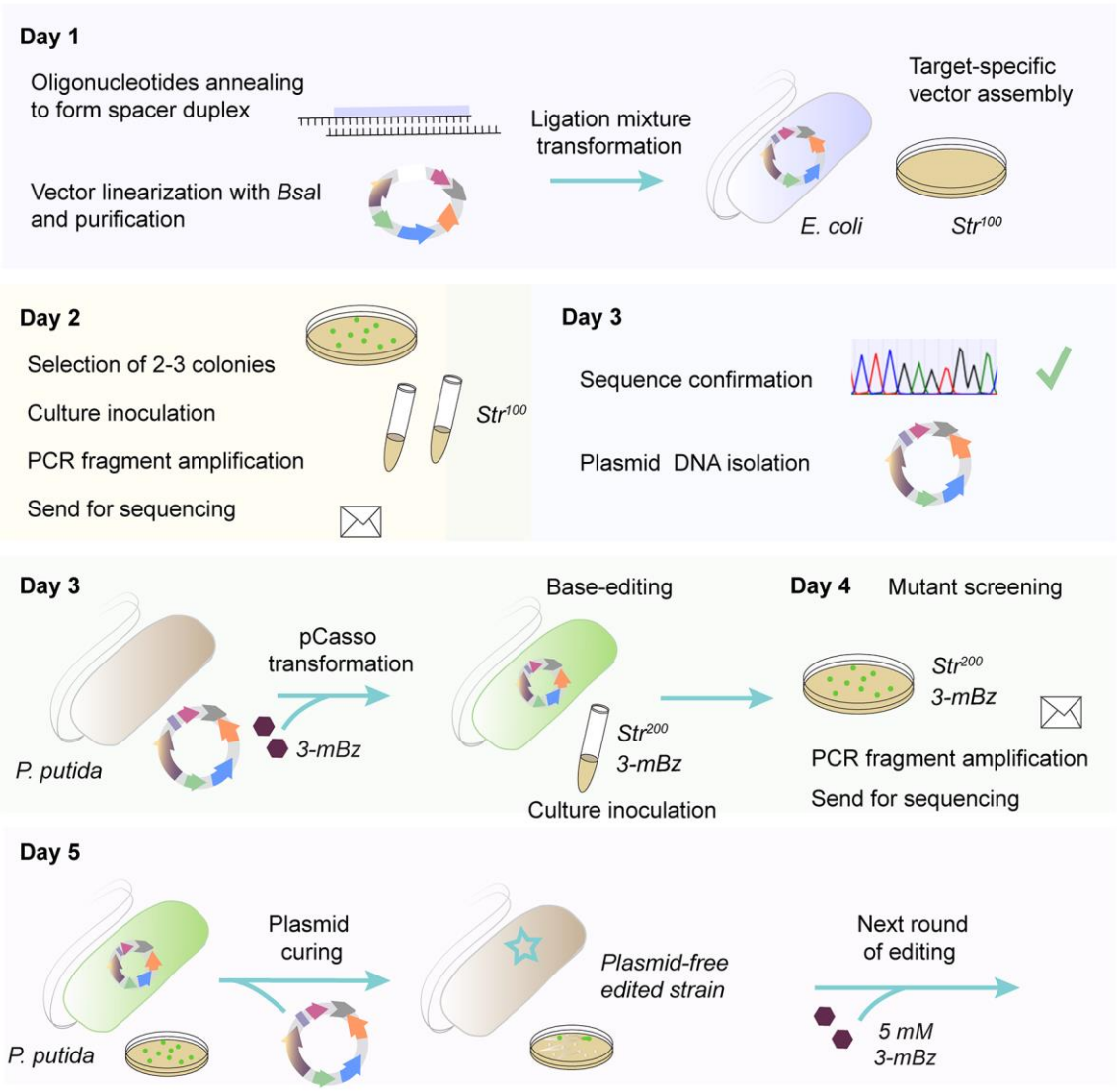

Day 1: Anneal single-strand DNA oligonucleotides by reverse cooling to form a double-stranded DNA spacer-insert array and clone it into the respective vector. Transform a suitable cloning *E. coli* strain and incubate the plates overnight (with 100 μg mL^{-1} of streptomycin for selection, indicated at Str^{100}). **Day 2:** Inoculate two or three transformants in liquid LB medium cultures and grow the cultures overnight. Amplify the corresponding fragment by PCR and send the amplicons for sequencing for spacer verification. **Day 3:** Purify independent plasmids with verified sequence and transform them in *Pseudomonas* cells by electroporation. Incubate 10 μL of the transformed culture in 10 mL of LB medium under streptomycin selection (Str^{200}) with the addition of 2 mM 3-m*Bz* to ensure plasmid replication and efficient editing. **Day 4:** Restreak green fluorescent colonies (msfGFP^{+}) on LB plates with Str^{200} and 5 mM 3-*m*Bz. **Day 5:** Amplify the corresponding fragment containing the intended modification by PCR from at least 15

individual colonies and send for sequencing for base-editing verification. Restreak selected colonies by dilution on the agar plate with non-selective medium (LB medium) for plasmid curing. Next day, the cured (non-fluorescent) colonies can be picked under blue light in a transilluminator and inoculated for the next round of editing or further strain characterization.